**Atmospheric
Measurement
Techniques
Discussions**

Retrieval of aerosol mass load (PM$_{10}$) from MERIS/Envisat top of atmosphere spectral reflectance measurements

G. J. Rohen[1,*], W. von Hoyningen-Huene[1], A. Kokhanovsky[1], T. Dinter[1], M. Vountas[1], and J. P. Burrows[1]

[1]Institute of Environmental Physics (IUP), University of Bremen, Otto-Hahn-Allee 1, 28359 Bremen, Germany
[*]now at: Alfred-Wegener-Institute for Polar and Marine Research, Bussestr. 24, 27570 Bremerhaven, Germany

AMTD

3, 5429–5467, 2010

PM$_{10}$ from MERIS/Envisat

G. J. Rohen et al.

Title Page

Abstract	Introduction
Conclusions	References
Tables	Figures

◄◄ | ►►

◄ | ►

Back | Close

Full Screen / Esc

Printer-friendly Version

Interactive Discussion

G. J. Rohen et al.

Abstract

A retrieval of particulate matter concentration (PM$_{10}$) from satellite data is presented as well as improvements of the aerosol optical depth retrieval by the Bremen aerosol algorithm. The add-on retrieval of particulate matter uses the derivation of the effective radii from the Ångstroem exponents and an assumed log-normal size distribution function. The Ångstroem exponent is derived through the multi-channel approach using MERIS/Envisat data, and benefits from the fitting of a smooth spectral slope of aerosol optical depth and the surface reflectance. The advantage of the retrieval is that this retrieval of the aerosol mass, i.e., in particular the effective radius, is exclusively based on spectral information from satellite measurements, global aerosol models, and meteorological parameters. ECMWF Boundary layer height, humidity, temperature, and pressure data are used in the retrieval; a retrieval of PM inferred without meteorological information and a proper BRDF is shown to be not very promising.

Over the city of Hamburg, the aerosol optical depths agree within a standard deviation of 0.03 and 0.068 for all thirteen wavelengths between 412 and 885 nm, compared with AERONET and ground based air quality measurements; the particulate matter concentrations show agreement with a correlation factor of 0.64. In addition to the urban site of Hamburg, comparisons of PM$_{10}$ measurements over rural sites in Germany exhibit a correlation coefficient of 0.75.

1 Introduction

Atmospheric pollution due to natural and anthropogenic emissions of aerosols is now known to be a serious threat to human health due to respiratory and toxic adverse health effects. Studies estimated the increase of total mortality between 0.4 and 1% for each increase of 10 μg/m^3 in PM$_{10}$ concentration which mean for instance up to about 24 000 deaths in the USA alone each year (Pope III et al., 2002; Mokdad et al., 2004).

The US Environmental Protection Agency (EPA) introduced regulations and limits for the concentrations of particulate matter with diameters smaller than $10\,\mu g/m^3$ (PM_{10}) in 1987, and since 1999 also relating to $PM_{2.5}$ due to the more dangerous adverse respiratory health effects of these finer particles. Also since 1999, every country in the European Union has to provide a dense PM_{10} measurement system for urban agglomeration with more than 250 000 people (EC, 1997). PM_{10} concentrations are not allowed to exceed $50\,\mu g/m^3$ for 35 days per annum in Europe, and $40\,\mu g/m^3$ on yearly average. In Germany, 1224 measurement stations, maintained by the federal states and partly by the German Environmental Agency (UBA), measure PM_{10} concentrations in general every thirty minutes. In the future, the obligations are supposed to become more rigid and change also referring to $PM_{2.5}$.

Since approximately the same time in the last decade, different airborne and satellite observations are used for the determination of the aerosol optical depth over water, (e.g., Husar et al., 1997; Tanré et al., 1999; von Hoyningen-Huene et al., 2003; Kahn et al., 2007) and over land (e.g., Herman et al., 1997; King et al., 1999; Kaufman et al., 1997; Deuzé et al., 2001; von Hoyningen-Huene et al., 2003; Lee et al., 2006; Levy et al., 2007a,b) through which information about the aerosol mass load in the atmosphere and near the surface is hoped to be provided. Today, most of those retrievals provide aerosol optical depth information which can be validated easily, for instance through the AERONET sun photometer reflectance measurements (Holben et al., 2001). The quality of the retrievals of aerosol optical depth from satellite data is nevertheless variable (Kokhanovsky et al., 2007) since the inversion still depends on many assumptions and local models. Performing global aerosol retrievals is still a challenge. Kokhanovsky et al. (2007) gave an overview of most of current aerosol optical depth retrievals from space. Especially for so called mega-cities like Mexico City or Beijing, but also in order to fill measurement gaps in the national air quality surveillance systems, more accurately retrieved and validated aerosol optical depth raises the hope that observations from space could be a substantial supplement or even a replacement of the cost-effective ground and sometimes not objective measurement gauging

systems (e.g., Al-Saadi et al., 2005). The quality of the ground based air quality surveillance system is also known to be highly variable (Williams and Bruckmann, 2004).

Many approaches have been made to find a correlation between aerosol optical depth and the particulate matter mass concentration (e.g., Chu et al., 2003; Wang and Christopher, 2003; Kacenelenbogen et al., 2006; Gupta et al., 2006). Although good correlations have been found in some cases (e.g., Engel-Cox et al., 2006, for the Eastern USA), it is now obvious that the particulate matter mass concentration retrievals based only on the columnar aerosol optical depth is not sufficient to infer finally in accurate aerosol mass measurements (Uhlig and von Hoyningen-Huene, 1993). This is reasonable because a change of meteorological parameters like the planetary boundary layer height or the humidity of the air can cause a massive change of the mass concentration whereas aerosol optical depth is less affected by these parameters. Additionally, it is important to know the vertical distribution of the aerosol mass concentration profile when someone aims to infer the PM_x concentration above the surface.

To deduce reliable information about the PM_x mass load, retrievals have been done using additional assumptions about the consistency of the local aerosol or additional information from other ground or space based LIght Detection And Ranging (LIDAR) information about the size distribution of the aerosols, i.e., information about local aerosol model (Engel-Cox et al., 2006) or using models (Pelletier et al., 2007; Vidot et al., 2007; Levy et al., 2007a,b). Levy et al. (2007a) classified aerosols and their absorption properties, i.e., the single scattering albedo, on a global scale. Although the results are quite promising, those techniques are only successful for the region in which further information is added. A global retrieval of PM_x only based on the spectral information without assumptions of the observed matter is presently not available except very simple techniques which basically only assume a simple correlation of aerosol optical depth and PM_x and therefore do not provide a sufficient quality.

A possibility to validate or compare the retrieved PM_x results is essential to assess the capability of the retrieval for providing reliable PM_x mass concentrations. This is not as easy as in the case of validation of aerosol optical depth with, e.g., those measured

PM$_{10}$ from MERIS/Envisat

G. J. Rohen et al.

by AERONET stations. For instance, the definition of PM$_x$ is fairly different for different measurement techniques. The dense national air quality surveillance system in the USA as well as in the EU provides such a measurement system for comparison.

The Environment Protection Agency (EPA) already started an integrated decision support tool called the Three Dimensional Air Quality System (3-D-AQS) (Hoff et al., 2006) which is an extension of the Infusing Satellite Data into Environmental Applications (IDEA) inferring aerosol optical depth from the MODerate resolution Imaging Spectroradiometer (MODIS) satellite (Szykman et al., 1995). This example shows the public interest in space based PM$_x$ data. Similar tools to improve the air quality surveillance will certainly be developed also in Europe in the future.

In this paper, a technique to retrieve boundary layer PM$_{10}$ from the Medium Resolution Imaging Spectrometer (MERIS) (Baudin et al., 1991) on board the European Space Agency (ESA) Environmental satellite (ENVISAT) over land is introduced. The technique is based on spectral and meteorological information and on radiative transfer calculations. The presented approach profits by the large number of spectral channels (13) of the MERIS instrument. Those are used to deduce reliable Ångstroem-α coefficients through interpolation from seven channels in the visible and near infrared spectral range. After introducing the retrieval methodology, we will show comparisons of the aerosol optical depth measurements with those from AERONET and describe the advantages of the MERIS aerosol optical depth retrievals in more detail, in particular the upstream constraints which benefit substantially from the interpolation of the Ångstroem-α exponents over all wavelengths. Using this, a more accurate derived effective radius can be used to invert columnar aerosol optical depth into an adequate aerosol mass load, assuming a log-normal aerosol size distribution function. The dense national air quality surveillance measurements are used for a first statistical comparison of the retrieved results over Hamburg in 2006. The paper finally ends with a discussion about the capability of satellites to improve the quality of the national air quality measurements.

Title Page

Abstract | Introduction

Conclusions | References

Tables | Figures

◄ | ►

◄ | ►

Back | Close

Full Screen / Esc

Printer-friendly Version

Interactive Discussion

2 MERIS aerosol optical depth retrievals with PMBAER

The basis of the presented PM_{10} retrieval is spectral aerosol optical depth as retrieved from the MERIS/ENVISAT data with the Bremen AErosol Algorithm (BAER) (von Hoyningen-Huene et al., 2003). BAER, including the add-on for the retrieval of
5   particulate matter, is hereafter called Particulate Matter Bremen Aerosol Retrieval (PM-BAER).

PMBAER basically subtracts the reflectance caused by Rayleigh scattering and surface reflection from the total reflectance; the result is assumed to be caused by aerosols. Radiative transfer calculations relate from this aerosol reflectance to the
10   aerosol optical depth.

The exact determination of the Ångstroem-α coefficient and its relationship to the effective radius is one of the largest possible error sources since only a slight change of the slope results in massive changes of the effective radius. The effective radius is the initial point for the derivation of the mass load. Although other visible/near infrared
15   instruments are suitable as input for the PMBAER algorithm, the MERIS instrument provides a larger number of channels which stabilize the characteristic determination and interpolation of the Ångstroem-α coefficients at each wavelength.

This 68.5° (swath width) nadir viewing MERIS imager (Baudin et al., 1991) consists of fifteen so called ocean color bands which are selectable across the range between
20   390 and 1040 nm. The bandwidth is programmable between 2.5 and 30 nm and the accuracy of the bands provides radiance measurements typically with signal-to-noise values in the range of 1700. For our retrieval, data from channels with bandwidth of 10 nm have been used. MERIS's swath width is 1150 km, and global coverage is reached within about three days at the equator and above mid-latitudes within almost
25   two days. The spatial resolution is 1040×1200 m, over land and at the coasts data with a resolution of 260×300 m are also available. This high resolution may be of importance for the retrieval of PM_x because emission sources in the street canyons

and industrial areas are mostly of a very small extent. A meaningful comparison with the ground based measurements may become difficult to perform.

For the retrieval of aerosol optical depth from the MERIS radiances, the top-of-atmosphere reflectance is derived through extraterrestrial irradiance as measured by the satellite and an air mass factor. Currently, thirteen wavelengths are used for the retrieval over water and seven channels for the retrieval over land (412.5 nm; 442.4 nm; 489.7 nm; 509.7 nm; 559.6 nm; 619.6 nm; 664.6 nm). For retrievals over water, 680.9 nm, 708.4 nm, 753.4 nm, 778.4 nm, 864.8 nm, and 884.6 nm are used additionally.

PMBAER subtracts the Rayleigh path reflectance using a parameterization for shorter wavelengths (Deepak et al., 1980) and a radiative transfer calculation for longer wavelengths (Nakajima and Tanaka, 1988). Pressure is obtained through a 30 arc seconds resolute digital elevation model (Row et al., 1995), and temperature is taken from ECMWF models.

In addition to a threshold criterion for clouds derived from the minimum cloud reflectance (Kokhanovsky, 2001) (top-of-atmosphere reflectance greater than 0.2), two additional criteria are used to detect clouds; the first is based on the variability; clouds are detected if the standard deviation of the top of atmosphere reflectance (5 × 5 pixel) divided by the mean is greater than 0.05. Furthermore, clouds are also detected if the fraction of reflectance at 412 nm and at 440 nm is smaller than 1.13.

For the separation of the surface reflectance, a weighted mixing of bare soil and green vegetation and a normalized differential vegetation index (NDVI) at 670 and 865 nm is considered which is also fitted to a smooth Ångstroem-α exponent (von Hoyningen-Huene et al., 2006b). Spectral reflectance measurements from the Compact Airborne Spectral Imager (CASI) and extensions from the CAMELEO database are used for this purpose. In order to consider the viewing angle range of the MERIS swath (totally about 76°), a bidirectional surface reflectance distribution function, (BRDF) was implemented (see Fig. 1 with a fixed azimuth angle of 170°). The BRDF semi-empirical model was taken from Sinyuk et al. (2006), parameters for the

G. J. Rohen et al.

anisotropy and for the backscatter have been found empirically through comparisons with AERONET data over Hamburg; no retrieval of the parameters has been done. This model was already shown to work for different surfaces (Sinyuk et al., 2006) and was also used for MERIS/PMBAER retrievals over desert surfaces (Dinter et al., 2009).

5   However, the usage of a surface BRDF is essential and cannot be omitted; this is demonstrated by a first brief comparison (Fig. 2) of MERIS aerosol optical depth from a set of sixteen measurements over Germany compared to measurements from AERONET over Hamburg. Mean bias was improved from 0.091 to 0.017 and standard deviation from 0.0841 to 0.075. Applied MERIS scenes will also be used later for the

10 validation of PM$_{10}$.

As mentioned above, PMBAER finally uses look-up-tables to deduce the aerosol optical depth $\tau(\lambda)$ from the top-of-atmosphere reflectance $R(\lambda)$, derived by a radiative transfer model (Nakajima and Tanaka, 1988),

$$\tau(\lambda) = \frac{R(\lambda,\mu,\Phi,\mu_0,\Phi_0)}{P(\lambda,\mu,\Phi,\mu_0,\Phi_0)} \frac{4\mu\mu_0}{\omega_0(\lambda)} \tag{1}$$

15 where (μ,Φ) and (μ_0,Φ_0) are satellite and solar zenith and azimuth angles, respectively, $P(\lambda,\mu,\Phi,\mu_0,\Phi_0)$ is the aerosol phase function and $\omega_0(\lambda)$ is the single scattering albedo. The exact determination of the correct phase function is crucial because of the non-linear dependence of the retrieved aerosol optical depths on this function. In contrast to the phase function, the single scattering albedo does not vary to that extent.

20 For our retrievals, ω_0 was set to 1 (see for instance LACE-98, Ansmann et al., 2002, where a mean ω_0 of 0.98 was measured).

Experimental scattering parameters have been taken from the Lindenberg Aerosol Characterization Experiment 1998 (LACE-98) (Ansmann et al., 2002), phase functions and single-scattering albedo as derived through data from sun and sky radiometers

25 and through the Coupled Inversion Radiative Transfer (CIRATRA) retrieval algorithm (von Hoyningen-Huene and Posse, 1997). This phase function as used in PMBAER as well as phase functions as provided by the AERONET station in Hamburg for different inversion modes and days are shown in Fig. 3.

The agreement of PMBAER aerosol optical depth as retrieved from data from Sea-WiFS, SCIAMACHY and MERIS satellites with AERONET and other satellites has already been shown in several studies (von Hoyningen-Huene et al., 2003, 2007a; Kokhanovsky et al., 2007), and also in applications like observations of Russian forest fires (Lee et al., 2003) or over Korea (Lee et al., 2006). Measurements over water as well over desert ground have also been successfully performed (von Hoyningen-Huene et al., 2006b; Dinter et al., 2009).

For this study, ten cloud-free days over Hamburg AERONET station mainly in 2006 have been taken for comparisons of the aerosol optical depth spectra (Fig. 4). Those days will be also used later for comparisons of the retrieved PM$_{10}$ with measurements of the air quality surveillance stations in Hamburg in order to assess the quality of the particulate matter retrieval. The comparisons reveal a standard deviation between 0.032 and 0.068, depending on the wavelength (see Table 1). For longer wavelengths, an increasing offset can be observed.

3 PM$_{10}$ retrieval methodology

The first task of the retrieval of particulate matter from optical depth is the determination of a relationship between τ and the aerosol mass.

Let a be the radius of the single aerosol particle which is assumed to be spherical and $Q_{\text{ext}}(a, \lambda, n)$ the dimensionless extinction efficiency which has been calculated through Mie theory (Lentz, 1976) (see also shape of $Q_{\text{ext}}(a, \lambda, n)$ and the limitation related to the size parameter by Kokhanovsky et al., 2006). $n = n(\lambda)$ denotes the refraction index of the particle which is taken from the Optical Properties of Aerosols and Clouds (OPAC) database (Hess et al., 1998).

The extinction within the objected air mass column has to be integrated over the particle distribution $\frac{df}{da}$ and the height z (absorption is neglected in these equations, $\varpi_0 = 1$),

$$\tau(\lambda) = N \int_0^{TOA} \int_0^\infty \pi a^2 Q_{ext}(a,\lambda,n) \frac{df(a,z)}{da} da\, dz, \tag{2}$$

where N is the number of particles in the observed air mass. Substitution through

$$\frac{dm}{da} = \frac{4\pi a^3}{3} \rho \frac{df}{da}, \tag{3}$$

where ρ denotes the humidity corrected density, leads finally to the wanted relationship between τ and the mass load,

$$\tau(\lambda) = N \int_0^{TOA} \int_0^\infty \frac{3}{4\rho a} Q_{ext}(a,\lambda,n) \frac{dm(a,z)}{da} da\, dz. \tag{4}$$

Under consideration of a vertically homogeneously distributed aerosol concentration $\frac{dm(a,z)}{da}$, this relationship can be written as

$$\tau(\lambda) = \frac{MH\langle C_{ext}(\lambda) \rangle}{\rho\langle V \rangle}. \tag{5}$$

M is the searched aerosol mass concentration, H denotes the aerosol layer. In the retrieval, 90% of the aerosol is assumed to be within the boundary layer height which is routinely provided by the European Center for Medium-Range Weather Forecasts (ECMWF). This estimate is strictly speaking only valid for continental sites.

$$\langle V \rangle = \frac{4\pi}{3} \int_0^\infty a^3 f(a) da \tag{6}$$

is the average volume of the particles.

$$\langle C_{ext} \rangle = \pi \int_0^\infty a^2 Q_{ext} f(a) da \tag{7}$$

is the average extinction cross section and $f(a)$ is the normalized lognormal distribution function which was chosen to be mono-modal for the retrieval of PM$_{10}$ concentration.

Printer-friendly Version

Interactive Discussion

The derivation of the aerosol mass M can therefore be written as

$$M = \gamma(f(a), \lambda)\tau \,, \tag{8}$$

where

$$\gamma(f(a), \lambda) = \frac{\rho \langle V \rangle}{H \langle C_{ext} \rangle} \,. \tag{9}$$

It should be noted that γ is not a constant but a function of wavelength λ and size distribution $f(a)$. Several groups already used Eq. (9) (e.g., Griggs, 1975, 1979; Fraser, 1976; Gassó and Hegg, 1997, 2003; Fraser et al., 1984; Kaufman et al., 1990; Mishchenko et al., 2002; Levy et al., 2007b). For the retrieval of coarse mode (PM$_{10}$) particles, a lognormal size distribution

$$f(a) = \frac{1}{\sigma a \sqrt{2\pi}} e^{-0.5\sigma^{-2} \ln^2 \left(\frac{a}{\mu} \right)} \tag{10}$$

is assumed, where σ is the half-width and μ the mean particle radius which is correlated with the effective radius a_{eff} through the division of the volume by the surface integral

$$a_{eff} = \frac{\int_0^\infty a^3 f(a)\,da}{\int_0^\infty a^2 f(a)\,da} \,. \tag{11}$$

Equation (11) can be adequately parameterized by

$$a_{eff} = \mu \exp(-2.5\sigma^2) \tag{12}$$

where $\sigma = 0.832\,\mu m$ and a is limited to less than $20\,\mu m$ (Kokhanovsky et al., 2006). This parameterization is used in PMBAER for fast retrievals. A typical effective radius of $0.282\,\mu m$, for instance, corresponds to a mean particle radius of $0.05\,\mu m$. To expand or specify the retrieval of different aerosol radii, e.g. PM$_{2.5}$, the size distribution function $f(a)$ can be modified adequately (see also Levy et al., 2007a). At last, it should be noted that this methodology has several uncertinties. For instance, the size distribution

could be variable as well the single-scattering-albedo ω_0. A detailed study about the sensitivity of the methodology is outstanding and has to be done in the future.

The effective radius can now readily be derived through the respective Ångstroem-α exponent

$$\alpha = \frac{-\ln\left(\frac{\tau(\lambda)}{\tau(\lambda_0)}\right)}{\left(\frac{\lambda}{\lambda_0}\right)} , \tag{13}$$

see Fig. 5. The top-of-atmosphere reflectance at wavelength λ is derived from the MERIS radiances $L(\lambda)$ by

$$R_\lambda^{\text{TOA}} = \frac{\pi L(\lambda) M_0}{E_0} . \tag{14}$$

M_0 is the air mass factor and E_0 the top-of-atmosphere irradiance at wavelength λ. The air mass factor depends on meteorological parameters like temperature and pressure.

Figure 5 shows the correlation which is used to infer the effective radius from the Ångstroem-α exponent. For the derivation of this correlation, Mie calculations (Lentz, 1976) using SeaWiFS and OPAC measurements (Hess et al., 1998) have been done.

The interpolated curve is described by the function

$$a_{\text{eff}} = 0.856 - 2.794\alpha + 9.699\alpha^2 - 18.157\alpha^3 + 11.792\alpha^4 . \tag{15}$$

It is very difficult to obtain reliable effective radii if α is less than 0.16, due to the large slope. In this case, the effective radius is set to 1.7 µm in the retrieval.

The multi-channel spectral information from MERIS allows one to infer not only an accurate aerosol optical depth as described in the last section, but also leads to a more accurate effective radius than in the case of using the aerosol optical depth and Ångstroem-α exponents from only a few channels which at last makes additional information, e.g., from other ground based measurements or models dispensable. However, for increasing bias as currently observed (see Fig. 4) this would result in a smaller

Ångstroem-α coefficient and therefore smaller effective radii and particulate matter concentrations.

First results of PM$_{10}$ retrievals without inclusion of the meteorology have been shown for a MERIS observation (von Hoyningen-Huene et al., 2006a) and from retrievals above Moscow from SeaWiFS data (Kokhanovsky et al., 2006). The retrieval presented here consists of the routine inclusion of meteorology data like the boundary layer height and humidity as well as improvements of the surface model via a Bidirectional Reflectance Distribution Function (BRDF). In the retrieval, boundary layer height and temperature data from ECMWF have been applied. A correction of particle size and density has been done using ECMWF humidity data.

Due to the different definitions of PM$_x$ by the national air quality measurement devices which use the ISO standard, an adjustment of the PM$_{10}$ definition towards the definition of the ground based measurements has be done in order to enable a comparison. the national air quality measurement devices assume not a sharp cutoff, but a smooth filter function over the 10 μm border (Fig 6). In the MERIS retrievals, a cut-off for the integration of the aerosol mass is assumed to be at 20 μm.

The effect of this weighting by the ISO filter function is negligible for small radii (see Fig. 7), but is large for larger particles (about 65% for particles with a size of 5 μm).

This means that the PM$_{10}$ mass load as retrieved by MERIS/PMBAER is generally larger than those of the ground based measurements. However, an adequate conversion is also done in PMBAER which can also be used for sites with sea aerosols or dust events.

The introduced meteorological and definition corrections have large effects on the retrieval results and are comparable to those effects resulting from large changes of the aerosol optical depth.

In the retrieval, 90% of the aerosol layer is assumed to be within the boundary layer height. This correlation was confirmed through CALIPSO LIDAR measurements, even for strong biomass burning injections (Labonne et al., 2007). Labonne et al. (2007) also showed that this assumption cannot be made in areas of strong changing boundary

layer height, e.g., at the coast. However, for most of the continental areas, the boundary layer height is therefore linearly correlated with the aerosol optical depth through Eq. (5). For usage in the PM$_{10}$ retrieval, the boundary layer height was interpolated to the MERIS local overflight time of about 10:00 (for the exact Envisat local overflight times see Rohen et al., 2008). The diurnal change of the boundary layer height increases in the morning by about 300 m per hour until the maximum is reached about noon (Baars, 2007). Following Eq. (5), such a change would imply a change of the PM$_{10}$ by a factor in some cases greater than approximately three. For instance, the boundary layer height varied between 1000 and 2500 m on 12 June 2006 over Germany (see Fig. 12).

The variation of the boundary layer height in Europe is even larger and cannot be neglected in PM$_x$ retrievals. This also shows that meteorological parameters can affect the retrieval results to the same or even larger extent than the aerosol optical depth itself.

3.1 Humidity correction

Due to condensation and evaporation effects, particle size, density, and shape, as well as the refractive index and the particle size distribution function are all affected by ambient humidity. This again causes changes of the optical and radiative transfer properties, e.g. the Ångstroem-α coefficients (Schuster et al., 2006). The particles become larger and more spherical, and their density decreases with humidity.

The Hänel (1976) model is commonly used to estimate this correlation between humidity, scattering coefficient, and particle radius. A parameterization of the humidity dependence of radius and scattering coefficient can be given by

$$a(h) = a_{\text{dry}} \cdot (1 - h)^{-\epsilon} \tag{16}$$

and

$$\sigma(h) = \sigma_{\text{dry}} \cdot (1 - h)^{-\gamma} , \tag{17}$$

G. J. Rohen et al.

where h is the relative humidity (0. . . 1), a_{dry} the radius of the particle in dry state, σ the light scattering coefficient (dry state σ_{dry}), and ϵ and γ are size growth parameters (see Hänel, 1971, for explicit values). Through simple forming both equations can be combined to

$$\frac{a(h)}{a_{\text{dry}}} = \left(\frac{\sigma(h)}{\sigma_{\text{dry}}}\right)^{\frac{\gamma}{\epsilon}} . \tag{18}$$

Although these correlations are used frequently, they do not consider hysteresis effects; depending on the direction of the changing ambient conditions, the correlation is different. From measurements at cloud-free conditions, a downward motion of the particles from the cooler to the warmer atmospheric layers is expected. Thus, the ambient humidity is supposed to change in a decreasing way, i.e., the air becomes drier.

There are many discussions going on about these hysteresis effects, but, for instance, for increasing and decreasing humidity, a different correlation has been measured for different sites over Paris, (Randriamiarisoa et al., 2006). The findings for the measurements with increasing humidity agree with the Hänel model. For decreasing humidity, larger particle sizes have been found. Figure 8 shows the particle growth as derived following the Hänel model for average aerosols (ϵ=0.25), maritime and dust aerosols (ϵ=0.18), and for urban aerosols (ϵ=0.285). Measurements from Randriamiarisoa et al. (2006) and corresponding regression curves.

For the humidity range below h=0.4 and above 0.9, the Hänel model is used for the retrieval with ϵ=0.25. For humidity between 0.4 and 0.9 the parameterization

$$\frac{a(h)}{a_{\text{dry}}} = 2.0138 + 0.94(1-h) - 4.331(1-h)^2 \tag{19}$$

is used.

For instance, assuming a variability of humidity h of 0.3, this would cause a two times larger radius of the particle and therefore an eight times larger mass load if the density is assumed to stay constant.

According to the changing volume of the particle, the particle density was also corrected in the retrieval. The humidity correction is strictly valid only for the particles at the surface. Currently, a homogenous distribution of humidity is assumed for the particulate matter retrieval. Although there are many indications that this is valid within the aerosol layer, the humidity is supposed to decrease with altitude and therefore, an overestimation can be caused due to this simplification.

The temperature affects the Rayleigh correction and the derivation of the air mass factor. If the temperature increases, the Rayleigh correction becomes larger; the contribution to the reflectance from the aerosols is therefore smaller, i.e., the aerosol optical depth. In contrast to that, the effect on the air mass factor increases the aerosol optical depth, at least at small aerosol optical depth. At larger aerosol optical depth, the contribution of the aerosols enhances, and with increasing temperatures an increase of aerosol optical depth is also expected. Because of the linear dependence of the air mass factor on these parameters and their relatively small percental changes (say about 30 Kelvin relativ to 285 and about 20 mbar relative to 1013), both parameters have a smaller impact on the derivation of the aerosol optical thickness compared to humidity.

Near real time ECMWF model temperatures are now routinely inserted into the retrieval.

4   Results and discussion

Earlier validations of the MERIS PM$_{10}$ retrievals have already been shown for retrieved PM$_{10}$ over Germany for 13 October 2003 (von Hoyningen-Huene et al., 2006a, 2008); they showed close agreement. Successful validations of PM$_{2.5}$ retrieved with PMBAER with AERONET have already been shown for a small area of South Sweden (Glantz et al., 2009).

One of the most important parameters in the PM$_{10}$ retrieval methodology is the accurate determination of the Ångstroem-α exponent, i.e., the spectral slope of the aerosol

optical depth. This parameter – in combination with the assumed size distribution function around the inferred effective radius – determines the effective radius and therefore the mass concentrations by a factor with the power of three. Figure 9 shows the comparison of Ångstroem-α exponents as retrieved from MERIS/PMBAER and from the collocated AERONET station in Hamburg for ten cloud-free days in 2005 and 2006, as deduced from the aerosol optical depth between 440 and 675 nm. The shown exponents are equivalent to effective radii between 0.03 and 0.2 µm (see Fig. 9).

The AERONET Ångstroem-α-α coefficients seem to be a little high (see also Che et al., 2008). It should be noted here that this α-coefficient is only based on satellite data. Considering this, the results in Fig. 9 can be assessed as satisfying.

Figure 10 shows comparisons of PM$_{10}$ from MERIS/PMBAER and from the national air quality measurement stations in Hamburg for the same days. Additionally, the location is indicated – background, traffic, or industry.

In general, a good agreement between both measurements can be seen with the exception of three outliers who may be reasoned by their specific location at traffic and industry sites. Omitting those three outliers, a correlation coefficient of 0.64 is reached. With a spatial resolution of 1200 m, MERIS is not able to look into a street canyon, and this may be the same argument for the industry situated site. The correlation may be much improved by using the full resolution MERIS data. At all background sites, MERIS observations are close to the air quality measurements.

Aerosol retrievals over cities are known to be difficult because of the unequal and varying surface; additionally, pollution sources like traffic or industry sites are relatively small and not widely distributed.

The next Fig. 11 shows a validation of results of PMBAER with air quality measurements in rural sites in Germany on sixteen days in 2005 and 2006. The corresponding correlation coefficient is 0.75. Additionally, Fig. 11 shows the effect of the synergy of ECMWF boundary layer height data; without considering this meteorological parameter, no good correlation can be achieved. Humidity turned out to have a negligible effect in the retrieval of the same scenes; this is most likely due to the fact that these

scenes are chosen as sunny and cloud-free days. However, the retrieval can therefore be used for regional measurements.

Figure 12 shows the aerosol optical depth, effective radii, and inferred PM$_{10}$ concentration from MERIS measurements over Germany on 12 June 2006, a sunny and dry day. The aerosol optical depth on that day exhibits reasonable values, and the transition between land and coast is also reasonable, except at the Wadden Sea where the surface model does obviously not work properly. Hot-spots can be observed clearly, for instance the cities Hamburg or Munich or even smaller cities. Cloud patterns in the northeast are easily recognizable although they are hardly visible in the RGB pictures. Artefacts can also be identified at mountains, e.g., at the Alps, where retrieved aerosol optical depth is too large (air there should be cleaner in general); this is most likely due to inaccurate Rayleigh correction and must be investigated in the future.

Comparisons of the particulate matter concentrations will certainly be improved if higher resolution satellite data are used. The comparisons over Hamburg showed that basically good results can be obtained, with the exception of street canyons and singular air pollution, e.g., singular industry sites.

5 Conclusions

A novel add-on of the Bremen AErosol Retrieval (PMBAER) for the derivation of the particulate matter concentration within the boundary layer has been presented, as well as improvements of the PMBAER surface model with respect to the bidirectional reflectance distribution function. The multi-channel approach turned out to be very useful in order to determine an accurate spectral slope; the accurate retrieval of the effective radius only based on satellite data is therefore the advantage of the MERIS/PMBAER retrieval. The great benefit of the MERIS/PMBAER retrieval is the accurate retrieval of the effective radius – and this only based exclusively on satellite data which is novel for PM$_{10}$ retrievals. The transition to PM$_{2.5}$ can be done relatively readily by using an adequate size distribution function.

The introduction of a bidirectional reflectance distribution function turned out to be essential in order to improve the optical depth retrieval. In particular at the outer parts of the MERIS field-of-view, the surface reflectance tended to be underestimated and therefore the aerosol optical depth was overestimated.

The retrieval uses the synergy of highly resolved meteorological parameters like boundary layer height, humidity and temperature from ECMWF. We showed that a PM$_{10}$ retrieval without the insertion of meteorological parameters is in general not possible.

Aerosol optical depth and particulate matter concentrations over Hamburg and over Germany have been derived and compared to measurements of AERONET, and with measurements of the German Environmental Agency, respectively, for ten days in 2005 and 2006. The comparisons of optical depth for all wavelengths between 412 and 885 nm show standard deviations between 0.03 and 0.06. The spectral slope also agrees fairly well with the Ångstroem-α exponent as derived from the MERIS aerosol optical depth measurements at 440 and 675 nm. Over an urban site (Hamburg) a correlation coefficient of 0.64, and over rural sites in Germany, a correlation coefficient of even 0.75 is reached.

Although comparisons fit relatively well, several assumptions have been made: a fixed size distribution function, no absorption, etc. An investigation about the sensitivity of these assumptions has to be done in the future in more details. Comparisons are restricted to the city of Hamburg and rural sites of Germany and have been done only on basis of cloud-free scenes. Problems of the retrieval have been identified at mountains and at the Wadden Sea where the distinguishing between water and land surface is difficult.

Summarized, this paper introduced the methodology and shows that the algorithm can be used for PM$_{10}$ measurements over cities and over rural sites. PMBAER in combination with MERIS satellite data is therefore capable of providing comparable particulate matter measurements which may be useful for assimilation of the ground based air quality surveillance network.

References

Al-Saadi, J., Szykman, J., Pierce, R. B., Kittaka, C., Neil, D., Chu, D. A., Remer, L., Gumley, L., Prins, E., Weinstock, L., MacDonald, C., Wayland, R., Dimmick, F., and Fishman, J.: Improving national air quality forecasts with satellite aerosol observations, B. Am. Meteorol. Soc., 86, 1249–1261, 2005. 5432

Ansmann, A., Wandinger, U., Wiedensohler, A., and Leiterer, U.: Lindenberg Aerosol Characterization Experiment 1998 (LACE-98): overview, J. Geophys. Res.-Atmos., 107, 8129, doi:10.1029/2000JD000233, 2002. 5436

Baars, H.: Continuous monitoring of the planetary-boundary-layer depth with lidar, Master's thesis, Universität Leipzig, 2007. 5442

Baudin, G., Bessudo, R., Cutter, M. A., Lobb, D., and Bezy, J. L.: Medium Resolution Imaging Spectrometer (MERIS), in: Future european and japanese remote-sensing sensors and programs, in: Proceedings of the Meeting, Orlando, FL, 1–2 April 1991 (A93-20426 06-19), edited by: Slater, P. N., vol. 1490 of Presented at the Society of Photo-Optical Instrumentation Engineers (SPIE) Conference, 102–113, 1991. 5433, 5434

CEN: Air quality determination of the PM_{10} fraction of suspended particulate matter, reference method and field test procedure to demonstrate reference equivalence of measurement methods, Tech. Rep. Ref. No. EN12341:1998 E, CEN Central Secretariat for Standardization, Brussels, 1998. 5461

Che, H., Shi, G., Uchiyama, A., Yamazaki, A., Chen, H., Goloub, P., and Zhang, X.: Intercomparison between aerosol optical properties by a PREDE skyradiometer and CIMEL sunphotometer over Beijing, China, Atmos. Chem. Phys., 8, 3199–3214, doi:10.5194/acp-8-3199-2008, 2008. 5445

Chu, D. A., Kaufman, Y. J., Zibordi, G., Chern, J. D., Mao, J., Li, C., and Holben, B. N.: Global monitoring of air pollution over land from the Earth Observing System – Terra Moderate Resolution Imaging Spectroradiometer (MODIS), J. Geophys. Res.-Atmos., 108, 4661, doi:10.1029/2002JD003179, 2003. 5432

Deepak, A., Box, M. A., and Box, C. P.: Retrieval of aerosol size distributions from scattering and extinction measurements in the presence of multiple scattering, in: Remote sensing of atmospheres and oceans; Proceedings of the Interactive Workshop on Interpretation of Remotely Sensed Data, Williamsburg, VA, 23–25 May 1979, A81-45861 22-46, New York, Academic Press, Inc., Discussion, 95–112, 1980. 5435

Deuzé, J. L., Bréon, F. M., Devaux, C., Goloub, P., Herman, M., Lafrance, B., Maignan, F., Marchand, A., Nadal, F., Perry, G., and Tanré, D.: Remote sensing of aerosols over land surfaces from POLDER-ADEOS-1 polarized measurements, J. Geophys. Res., 106, 4913–4926, doi:10.1029/2000JD900364, 2001. 5431

Dinter, T., von Hoyningen-Huene, W., Burrows, J., Kokhanovsky, A., Bierwirth, E., Wendisch, M., Müller, D., Kahn, R., and Diouri, M.: Retrieval of aerosol optical thickness for desert conditions using MERIS observations during the SAMUM campaign, Tellus B, 61, 229–238, 2009. 5436, 5437

EC: Council Directive 1999/30/EC of 22 April 1999 relating to limit values for sulphur dioxide, nitrogen dioxide and oxides of nitrogen, PM and lead in ambient air, Tech. Rep. 1999/30/EC, European Comission, Brussels, 1997. 5431

Engel-Cox, J. A., Hoff, M. R., Rogers, R., Dimmick, F., Rush, A. C., Szykman, J., Al-Saadi, J., Chu, D. A., and Zell, E. R.: Integrating lidar and satellite optical depth with ambient monitoring for 3-dimensional particulate characterization, Atmos. Environ., 40, 8056–8067, 2006. 5432

Fraser, R. S.: Satellite measurement of mass of Sahara dust in the atmosphere, Appl. Optics, 15, 2471–2479, 1976. 5439

Fraser, R. S., Kaufman, Y. J., and Mahoney, R. L.: Satellite measurement of aerosol mass over land, in: Conference on Satellite/Remote Sensing and Applications, Clearwater Beach, FL, 25–29 June 1984, Preprints, A85-37726 17-47, Am. Meteorol. Soc., Boston, MA, 4–10, 1984. 5439

Gasso, S. and Hegg, D. A.: Comparison of columnar aerosol optical properties measured by the MODIS airborne simulator with in situ measurements: a case study, Atmos. Environ., 66, 138–152, 1997. 5439

Title Page

Abstract | Introduction

Conclusions | References

Tables | Figures

◄◄ | ►►

◄ | ►

Back | Close

Full Screen / Esc

Printer-friendly Version

Interactive Discussion

Gassó, S. and Hegg, D. A.: On the retrieval of columnar aerosol mass and CCN concentration by MODIS, J. Geophys. Res.-Atmos., 108, 4010, doi:10.1029/2002JD002382, 2003. 5439

Glantz, P., Kokhanovsky, A., von Hoyningen-Huene, W., and Johansson, C.: Estimating $PM_{2.5}$ over Southern Sweden using space borne optical measurements, Atmos. Environ., 43, 5838–5846, 2009. 5444

Griggs, M.: Measurements of atmospheric aerosols over water using RTS-1 data, J. Air Pollut. Control Assoc., 25, 622–626, 1975. 5439

Griggs, M.: Satellite observations of atmospheric aerosols during the EOMET Cruise, J. Atmos. Sci., 36, 695–698, 1979. 5439

Gupta, P., Christophera, S. A., Wang, J., Gehrig, R., Leed, Y., and Kumar, N.: Satellite remote sensing of particulate matter and air quality assessment over global cities, Atmos. Environ., 40, 5880–5892, 2006. 5432

Hänel, G.: New results concerning the dependence of visibility on relative humidity and their significance in a model for visibility forecast, Atmos. Phys., 44, 137–167, 1971. 5443

Hänel, G.: The properties of atmospheric aerosol particles as function of the relative humidity at thermodynamic equilibrium with the surrounding moist air, Adv. Geophys., 19, 73–188, 1976. 5442, 5463

Herman, M., Deuzé, J. L., Devaux, C., Goloub, P., Bréon, F. M., and Tanré, D.: Remote sensing of aerosols over land surfaces including polarization measurements and application to POLDER measurements, J. Geophys. Res., 102, 17039–17050, doi:10.1029/96JD02109, 1997. 5431

Hess, M., Koepke, P., and Schult, I.: Optical properties of aerosols and clouds: the software package OPAC, B. Am. Meteorol. Soc., 79, 831–844, 1998. 5437, 5440

Hoff, R. M., Engel-Cox, J. A., Dimmick, F., Szykman, J. J., Johns, B., Kondragunta, S., Rogers, R., McCann, K., Chu, D. A., Torres, O., Prados, A., Al-Saadi, J., Kittaka, C., Boothe, V., Ackerman, S., and Wimmers, A.: 3D-AQS: a three-dimensional air quality system, in: Remote Sensing of Aerosol and Chemical Gases, Model Simulation/Assimilation, and Applications to Air Quality, edited by: Chu, A., Szykman, J., Kondragunta, S., Proceedings of the SPIE, Presented at the Society of Photo-Optical Instrumentation Engineers (SPIE) Conference, vol. 6299, p. 629901, doi:10.1117/12.677281, 2006. 5433

Holben, B. N., Tanré, D., Smirnov, A., Eck, T. F., Slutsker, I., Abuhassan, N., Newcomb, W. W., Schafer, J. S., Chatenet, B., Lavenu, F., Kaufman, Y. J., Castle, J. V., Setzer, A., Markham, B., Clark, D., Frouin, R., Halthore, R., Karneli, A., O'Neill, N. T., Pietras, C., Pinker, R. T.,

PM_{10} from MERIS/Envisat

G. J. Rohen et al.

Title Page

Abstract	Introduction
Conclusions	References
Tables	Figures

|◄ | ►|

◄ | ►

Back | Close

Full Screen / Esc

Printer-friendly Version

Interactive Discussion

Voss, K., and Zibordi, G.: An emerging ground-based aerosol climatology: aerosol optical depth from AERONET, J. Geophys. Res., 106, 12067–12098, doi:10.1029/2001JD900014, 2001. 5431

Husar, R. B., Prospero, J. M., and Stowe, L. L.: Characterization of tropospheric aerosols over the oceans with the NOAA advanced very high resolution radiometer optical thickness operational product, J. Geophys. Res., 102, 16889–16910, doi:10.1029/96JD04009, 1997. 5431

Kacenelenbogen, M., Léon, J.-F., Chiapello, I., and Tanré, D.: Characterization of aerosol pollution events in France using ground-based and POLDER-2 satellite data, Atmos. Chem. Phys., 6, 4843–4849, doi:10.5194/acp-6-4843-2006, 2006. 5432

Kahn, R. A., Garay, M. J., Nelson, D. L., Yau, K. K., Bull, M. A., Gaitley, B. J., Martonchik, J. V., and Levy, R. C.: Satellite-derived aerosol optical depth over dark water from MISR and MODIS: comparisons with AERONET and implications for climatological studies, J. Geophys. Res.-Atmos., 112, 18205, doi:10.1029/2006JD008175, 2007. 5431

Kaufman, Y. J., Ferrare, R. A., and Fraser, R. S.: Satellite measurements of large-scale air pollution – methods, J. Geophys. Res., 95, 9895–9909, 1990. 5439

Kaufman, Y. J., Tanré, D., Remer, L. A., Vermote, E. F., Chu, A., and Holben, B. N.: Operational remote sensing of tropospheric aerosol over land from EOS moderate resolution imaging spectroradiometer, J. Geophys. Res., 102, 17051–17068, doi:10.1029/96JD03988, 1997. 5431

King, M. D., Kaufman, Y. J., Tanré, D., and Nakajima, T.: Remote sensing of tropospheric aerosols from space: past, present, and future, B. Am. Meteorol. Soc., 80, 2229–2260, 1999. 5431

Kokhanovsky, A. A.: Reflection and transmission of polarized light by optically thick weakly absorbing random media, J. Opt. Soc. Am. A, 18, 883–887, 2001. 5435

Kokhanovsky, A. A., von Hoyningen-Huene, W., and Burrows, J. P.: Atmospheric aerosol load as derived from space, Atmos. Res., 81, 176–185, doi:10.1016/j.atmosres.2005.12.001, 2006. 5437, 5439, 5441

Kokhanovsky, A. A., Breon, F.-M., Cacciari, A., Carboni, E., Diner, D., di Nicolantonio, W., Grainger, R. G., Grey, W. M. F., Höller, R., Lee, K.-H., Li, Z., North, P. R. J., Sayer, A. M., Thomas, G. E., and von Hoyningen-Huene, W.: Aerosol remote sensing over land: a comparison of satellite retrievals using different algorithms and instruments, Atmos. Res., 85, 372–394, doi:10.1016/j.atmosres.2007.02.008, 2007. 5431, 5437

Discussion Paper | Discussion Paper | Discussion Paper | Discussion Paper | Discussion Paper |

AMTD

3, 5429–5467, 2010

PM$_{10}$ from MERIS/Envisat

G. J. Rohen et al.

Title Page

Abstract	Introduction
Conclusions	References
Tables	Figures

◄◄ | ►►

◄ | ►

Back | Close

Full Screen / Esc

Printer-friendly Version

Interactive Discussion

Labonne, M., Bréon, F.-M., and Chevallier, F.: Injection height of biomass burning aerosols as seen from a spaceborne lidar, Geophys. Res. Lett., 34, 11806, doi:10.1029/2007GL029311, 2007. 5441

Lee, K. H., Kim, J. E., Kim, Y. J., and von Hoyningen-Huene, W.: Impact of the smoke aerosol from Russian forest fires on the atmospheric environment over Korea during May 2003, Atmos. Environ., 39, 85–99, 2003. 5437

Lee, K. H., Kim, Y. J., and von Hoyningen-Huene, W.: Influence of land surface effects on MODIS aerosol retrieval using the BAER method over Korea, Appl. Optics, 15, 2813–2830, 2006. 5431, 5437

Lentz, W. J.: Generating Bessel functions in Mie scattering calculations using continued fractions, Appl. Optics, 15, 668–671, 1976. 5437, 5440

Levy, R. C., Remer, L. A., and Dubovik, O.: Global aerosol optical properties and application to moderate resolution imaging spectroradiometer aerosol retrieval over land, J. Geophys. Res.-Atmos., 112, 13210, doi:10.1029/2006JD007815, 2007a. 5431, 5432, 5439

Levy, R. C., Remer, L. A., Mattoo, S., Vermote, E. F., and Kaufman, Y. J.: Second-generation operational algorithm: retrieval of aerosol properties over land from inversion of moderate resolution imaging spectroradiometer spectral reflectance, J. Geophys. Res.-Atmos., 112, 13211, doi:10.1029/2006JD007811, 2007b. 5431, 5432, 5439

Mishchenko, M. I., Lacis, A. A., and Travis, L. D.: Absorption, Scattering, and Emission of Light by Small Particles, Cambridge University Press, Cambridge, 2002. 5439

Mokdad, A. H., Marks, J. S., Stroup, D. F., and Gerberding, J. L.: Actual causes of death in the United States, 2000, J. Am. Med. Assoc., 291, 1238–1245, 2004. 5430

Nakajima, T. and Tanaka, M.: Algorithms for radiative intensity calculations in moderately thick atmospheres using a truncation approximation, J. Quant. Spectrosc. Ra., 40, 51–69, 1988. 5435, 5436

Pelletier, B., Santer, R., and Vidot, J.: Retrieving of particulate matter from optical measurements: a semiparametric approach, J. Geophys. Res.-Atmos., 112, 6208, doi:10.1029/2005JD006737, 2007. 5432

Pope III, C. A., Burnett, R. T., Thun, M. J., Calle, E. E., Krewski, D., Ito, K., and Thurston, G. D.: Lung cancer, cardiopulmonary mortality, and long-term exposure to fine particulate air pollution, J. Am. Med. Assoc., 287, 1132–1141, 2002. 5430

Title Page

Abstract | Introduction

Conclusions | References

Tables | Figures

|◄ | ►|

◄ | ►

Back | Close

Full Screen / Esc

Printer-friendly Version

Interactive Discussion

Randriamiarisoa, H., Chazette, P., Couvert, P., Sanak, J., and Mégie, G.: Relative humidity impact on aerosol parameters in a Paris suburban area, Atmos. Chem. Phys., 6, 1389–1407, doi:10.5194/acp-6-1389-2006, 2006. 5443, 5463

Rohen, G. J., Savigny, C. v., Kaiser, J. W., Llewellyn, E. J., Froidevaux, L., López-Puertas, M., Steck, T., Palm, M., Winkler, H., Sinnhuber, M., Bovensmann, H., and Burrows, J. P.: Ozone profile retrieval from limb scatter measurements in the HARTLEY bands: further retrieval details and profile comparisons, Atmos. Chem. Phys., 8, 2509–2517, doi:10.5194/acp-8-2509-2008, 2008. 5442

Row, L. W., Hastings, D. A., and Dunbar, P. K.: TerrainBase Worldwide Digital Terrain Data – Documentation Manual, Tech. Rep. CD-ROM Release 1.0, National Geophysical Data Center, Boulder, Colorado, 1995. 5435

Schuster, G. L., Dubovik, O., and Holben, B. N.: Angstrom exponent and bimodal aerosol size distributions, J. Geophys. Res.-Atmos., 111, 7207, doi:10.1029/2005JD006328, 2006. 5442

Sinyuk, A., Dubovik, O., Holben, B., Eck, T. F., Breon, F.-M., Martonchik, J., Kahn, R., Diner, D. J., Vermote, E. F., Roger, J.-C., Lapyonok, T., and Slutsker, I.: Simultaneous retrieval of aerosol and surface properties from a combination of AERONET and satellite data, Remote Sens. Environ., 107, 98–108, 2006. 5435, 5436, 5456

Szykman, J., White, J., Pierce, B., Al-Saadi, J., Neil, D., Kittaka, C., Chu, A., Remer, L., Gumley, L., and Prins, E.: Utilizing MODIS satellite observations in near-real-time to improve AIRnow next day forecast of fine particulate matter, $PM_{2.5}$, in: Conference on Atmospheric Chemistry, 6th: Air Quality in Megacities, Seattle, WA, 11–15 January 2004, preprints, no. Paper 1.2. Reprint 3630 in B. Am. Meteorol. Soc., Boston, MA, 75–80, 1995. 5433

Tanré, D., Remer, L. A., Kaufman, Y. J., Mattoo, S., Hobbs, P. V., Livingston, J. M., Russell, P. B., and Smirnov, A.: Retrieval of aerosol optical thickness and size distribution over ocean from the MODIS airborne simulator during TARFOX, J. Geophys. Res., 104, 2261–2278, doi:10.1029/1998JD200077, 1999. 5431

Uhlig, E.-M. and von Hoyningen-Huene, W.: Correlation of atmospheric extinction coefficient with the concentration of particulate matter in a polluted urban area, Atmos. Res., 30, 181–195, 1993. 5432

Vidot, J., Santer, R., and Ramon, D.: Atmospheric particulate matter (PM) estimation from SeaWiFS imagery, Remote Sens. Environ., 111, 1–10, 2007. 5432

von Hoyningen-Huene, W. and Posse, P.: Nonsphericity of aerosol particles and their contribution to radiative forcing, J. Quant. Spectrosc. Ra., 57, 651–668, 1997. 5436

Title Page

Abstract | Introduction

Conclusions | References

Tables | Figures

|◀ | ▶|

◀ | ▶

Back | Close

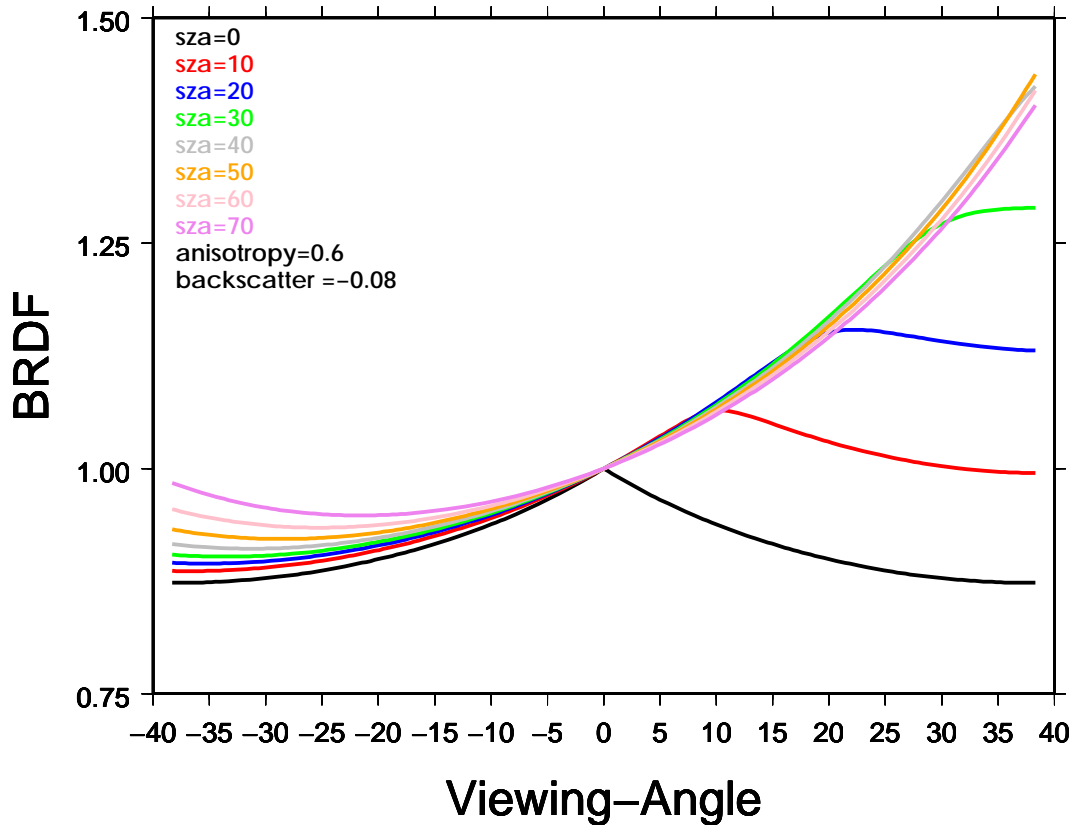Full Screen / Esc

Printer-friendly Version

Interactive Discussion

von Hoyningen-Huene, W., Freitag, M., and Burrows, J. P.: Retrieval of aerosol optical thickness over land surfaces from top-of-atmosphere radiance, J. Geophys. Res., 108, 4260, doi:10.1029/2001JD002018, 2003. 5431, 5434, 5437

von Hoyningen-Huene, W., Kokhanovsky, A., and Burrows, J. P.: Retrieval of particulate matter from MERIS observations, in: Proc. 6th Int. Symp. on Adv. Environ. Monitoring, Heidelberg, 2006a. 5441, 5444

von Hoyningen-Huene, W., Kokhanovsky, A. A., Burrows, J. P., Bruniquel-Pinel, V., Regner, P., and Baret, F.: Simultaneous determination of aerosol- and surface characteristics from top-of-atmosphere reflectance using MERIS on board of ENVISAT, Adv. Space Res., 37, 2172–2177, doi:10.1016/j.asr.2006.03.017, 2006b. 5435, 5437

von Hoyningen-Huene, W., Kokhanovsky, A. A., Wuttke, M. W., Buchwitz, M., Noël, S., Gerilowski, K., Burrows, J. P., Latter, B., Siddans, R., and Kerridge, B. J.: Validation of SCIAMACHY top-of-atmosphere reflectance for aerosol remote sensing using MERIS L1 data, Atmos. Chem. Phys., 7, 97–106, doi:10.5194/acp-7-97-2007, 2007a. 5437

von Hoyningen-Huene, W., Rohen, G., Dinter, T., Kokhanovsky, A. A., Vountas, M., Bovensmann, H., Burrows, J. P., and Wichmann-Fiebig, M.: Retrieval of Particulate Matter Concentration (PM_{10}) from MERIS observation and validation over Germany, in: Proc. of Envisat Symp. 2007, Montreux, Switzerland, ESA SP-636, 2007b. 5466

von Hoyningen-Huene, W., Kokhanovsky, A., and Burrows, J. P.: Retrieval of particulate matter from MERIS observations, in: Advanced Environmental Monitoring, edited by: Young, J. K. and Platt, U., Springer Publ., Dordrecht, The Netherlands, 190–202, 2008. 5444

Wang, J. and Christopher, S. A.: Intercomparison between satellite-derived aerosol optical thickness and $PM_{2.5}$ mass: implications for air quality studies, Geophys. Res. Lett., 30, 4–1, 2003. 5432

Williams, M. and Bruckmann, P.: A report on guidance to the member states on PM_{10} monitoring and inter-comparisons with the reference method, Tech. rep., EC Working Group on Particulate Matter, London, Venice, 2004. 5432

Title Page

Abstract | Introduction

Conclusions | References

Tables | Figures

|◄ | ►|

◄ | ►

Back | Close

Full Screen / Esc

Printer-friendly Version

Interactive Discussion

Table 1. Offsets and standard deviations for the comparisons of aerosol optical depth over Hamburg for different wavelengths for ten cloud-free days in 2006 (see Fig. 4).

λ	Bias, Std.-Dev.	λ	Bias, Std.-dev.
412.5	0.003 ± 0.056	680	0.045 ± 0.052
443	0.009 ± 0.045	708	0.050 ± 0.056
490	0.009 ± 0.034	753	0.047 ± 0.056
510	0.013 ± 0.032	778	0.048 ± 0.059
560	0.035 ± 0.045	865	0.056 ± 0.067
620	0.039 ± 0.040	885	0.054 ± 0.068
665	0.040 ± 0.050		

Fig. 1. BRDF as used for the retrieval of aerosol optical depth over Germany for different solar zenith angles (Sinyuk et al., 2006).

Title Page

Abstract | Introduction

Conclusions | References

Tables | Figures

|◄ | ►|

◄ | ►

Back | Close

Full Screen / Esc

Printer-friendly Version

Interactive Discussion
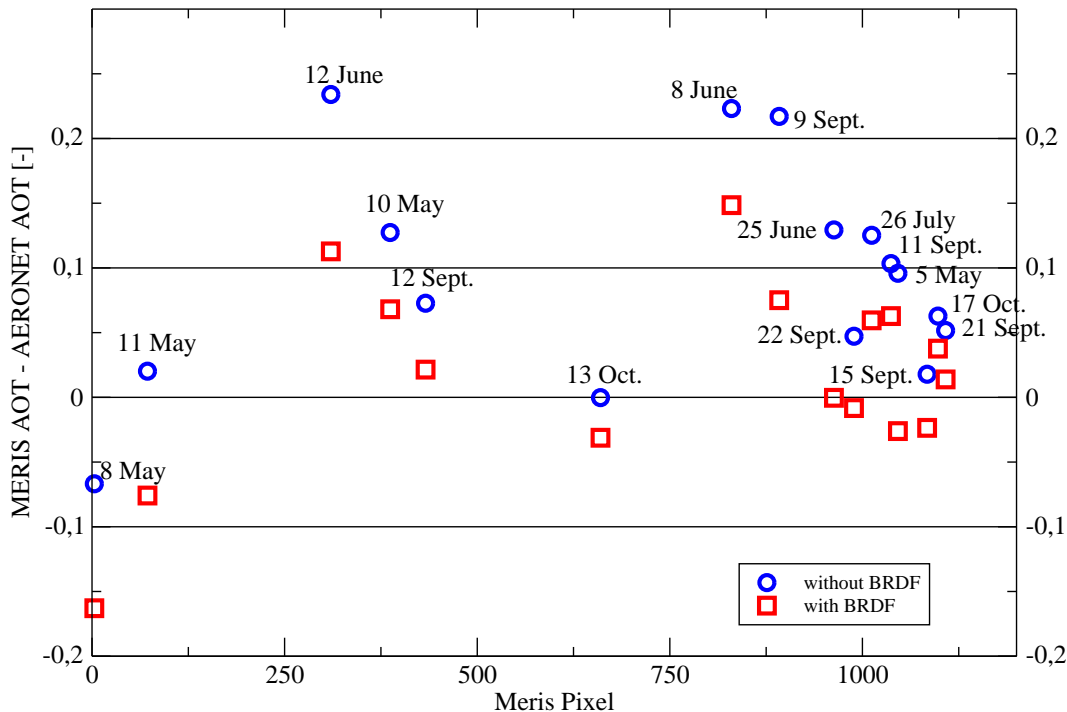
Fig. 2. Differences between MERIS (with and without BRDF effects) and AERONET aerosol optical depth measurements at 440 nm over Hamburg for sixteen collocated measurements at cloud free days in 2006. Pixels are given at the axis of abscissae in order to make clear the possible dependence on the viewing angle. Dates are given in order to enable a seasonal classification; retrievals in the summer seem to be worse than those in autumn with larger scattering angles; this is a typical BRDF effect.

Discussion Paper | Discussion Paper | Discussion Paper | Discussion Paper |
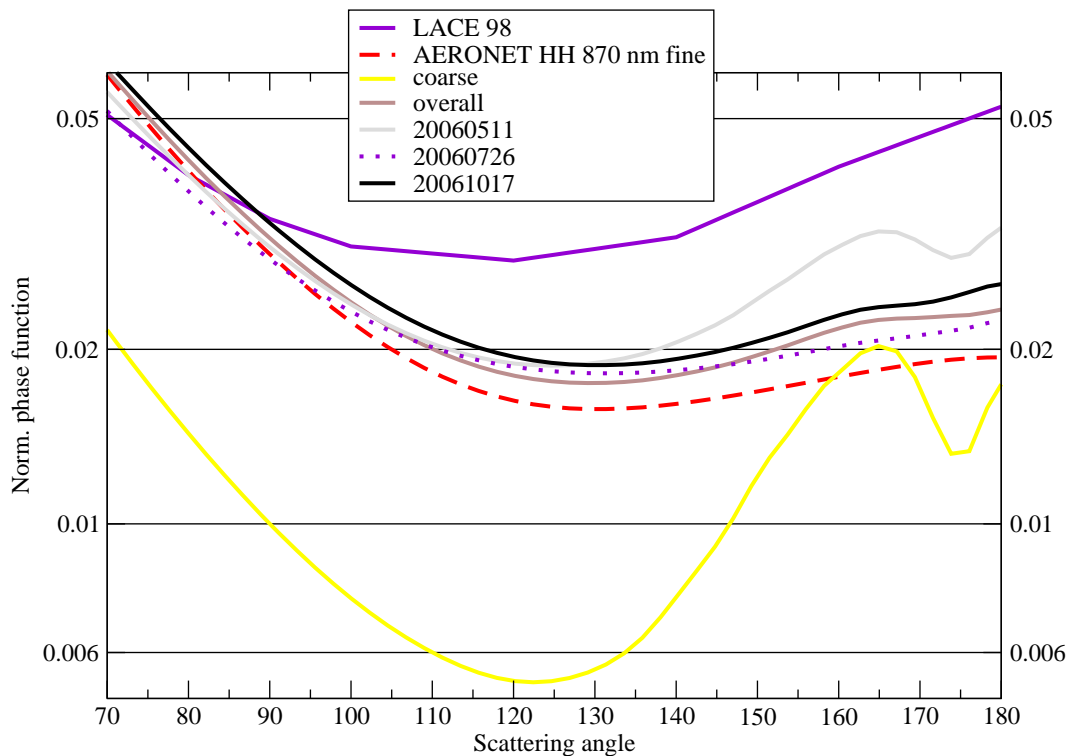
Fig. 3. Phase functions as derived from the LACE-98 experiment, phase functions at 870 nm for fine, coarse and overall modes as provided by AERONET in Hamburg on 13 October 2005 as well as overall phase functions for three other days in 2006 from AERONET Hamburg. Comparisons with phase functions at 440 and 1020 nm are similar.

Title Page

Abstract | Introduction

Conclusions | References

Tables | Figures

|◄ | ►|

◄ | ►

Back | Close

Full Screen / Esc

Printer-friendly Version

Interactive Discussion
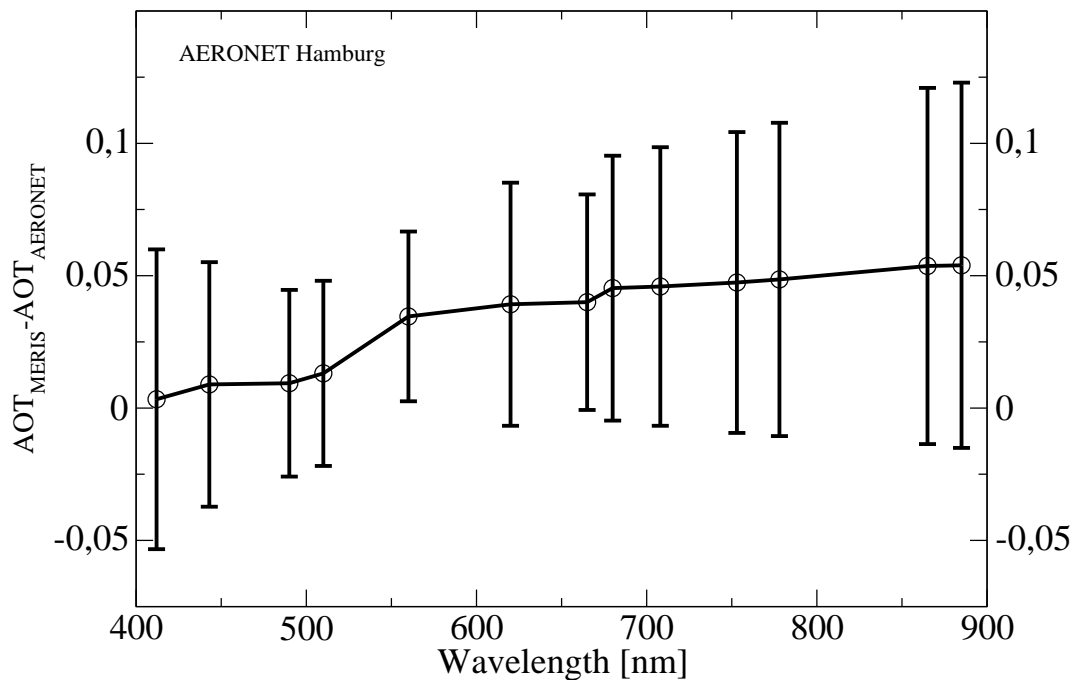
Fig. 4. Statistical comparison of ten collocated MERIS/PMBAER measurements of aerosol optical depth with AERONET over Hamburg. AERONET optical depths have been interpolated to the wavelengths as used for the retrieval. Bars indicate the standard deviation. See Table 1 for exact values.

Title Page

Abstract | Introduction

Conclusions | References

Tables | Figures

|◄ | ►|

◄ | ►

Back | Close

Full Screen / Esc

Printer-friendly Version

Interactive Discussion
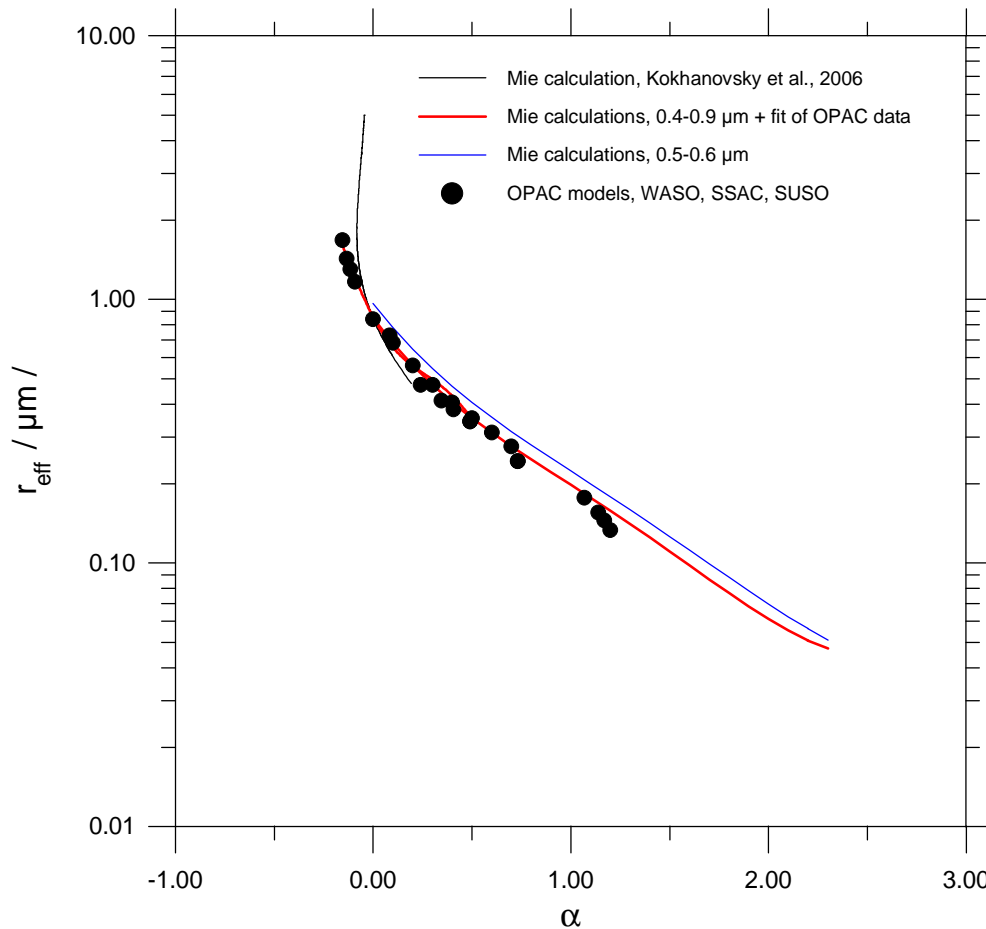
Fig. 5. Correlation between Ångstroem-α coefficient and effective radius as retrieved from Mie calculations as used in the retrievals and from improved correlations as interpolated from OPAC measurements.
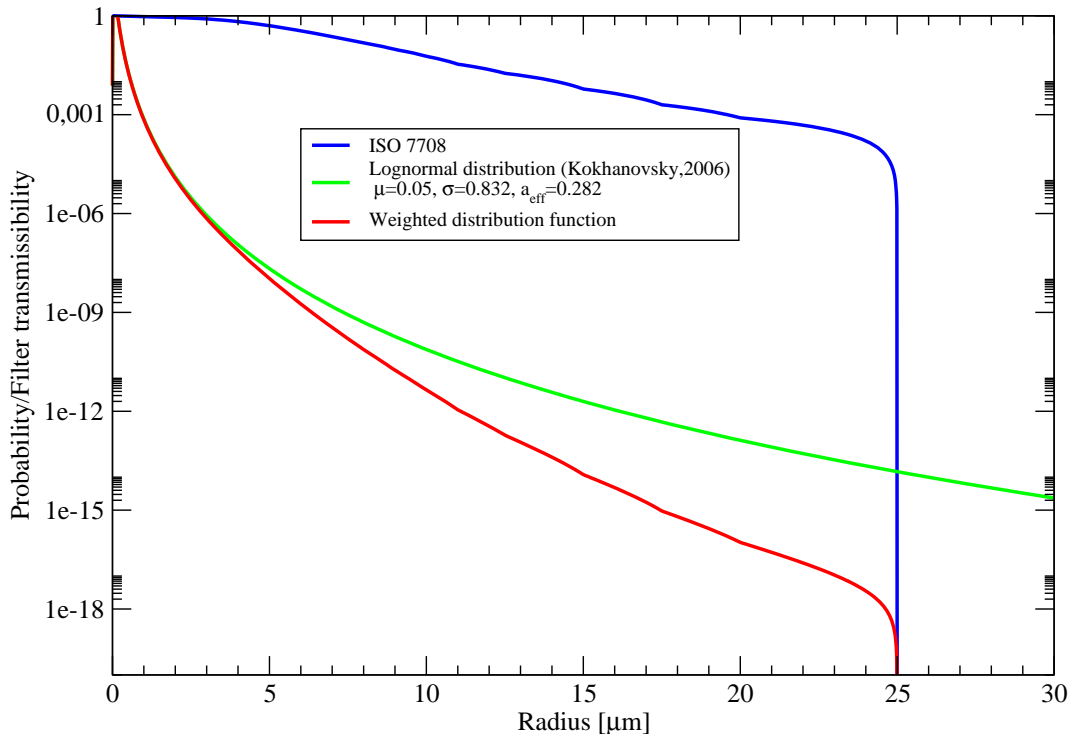
Fig. 6. Filter functions for the conversion between the different definitions of particulate matter mass load. The green line indicates the log-normal distribution function as used in PMBAER for an effective radius of 0.282 µm, the blue line indicates the filter function as provided by the European Standard CEN following ISO (CEN, 1998). The red curve denotes the weighted distribution function which is a folding of the log-normal distribution with the ISO weighting function.

Title Page

Abstract | Introduction

Conclusions | References

Tables | Figures

|◄ | ►|

◄ | ►

Back | Close

Full Screen / Esc

Printer-friendly Version

Interactive Discussion
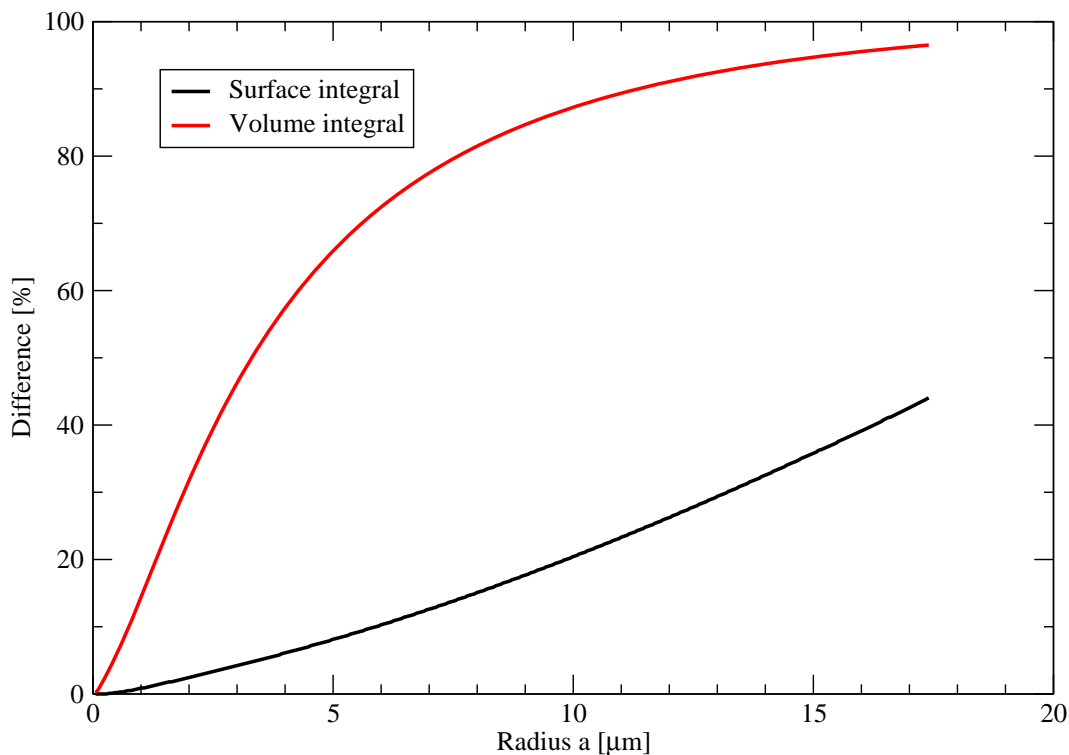
Fig. 7. Differences for the surface and volume integral (equivalent to the aerosol mass load) between the ISO definition of PM$_{10}$ and those using the log-normal distribution with a cut-off at 20 µm (see Eq. 10).
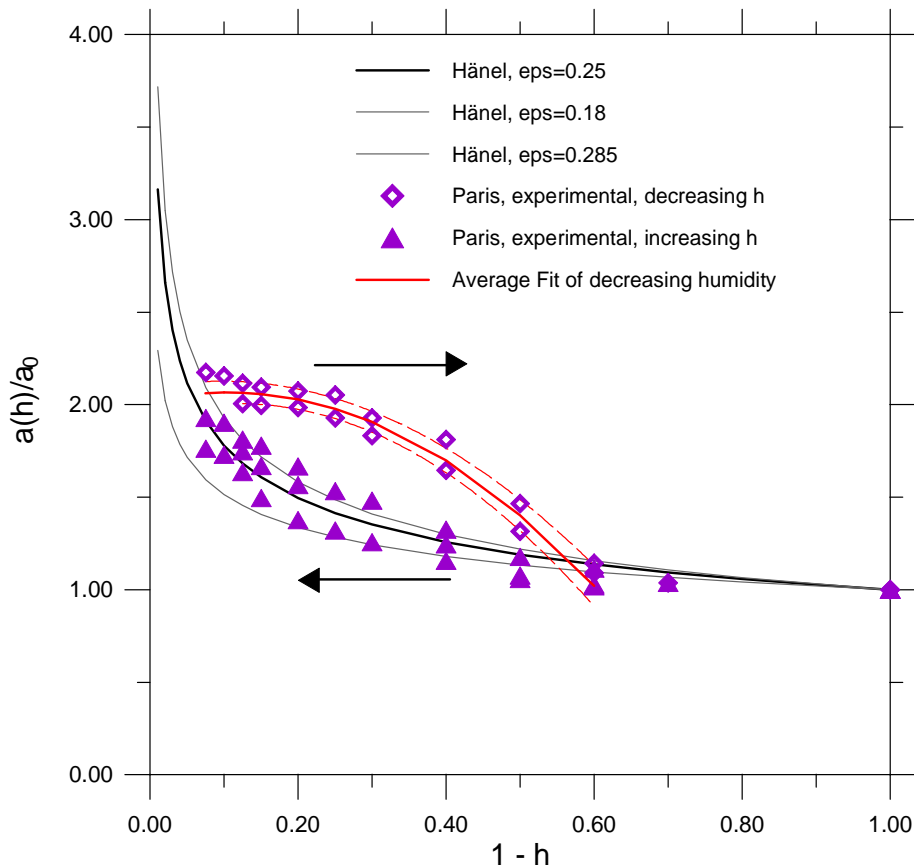
Fig. 8. Correlation between relative humidity (note the abscissa $1-h$) and particle growth as derived through the Hänel (1976) model and measurements over Paris (see Randriamiarisoa et al., 2006 for the setups of different measurements – indicated with the same symbols – during times of increasing and decreasing humidity). For the PM_{10} retrieval, the parameterization of Eq. (19) as indicated by the solid red line, is used.

Title Page

Abstract | Introduction

Conclusions | References

Tables | Figures

|◄ | ►|

◄ | ►

Back | Close

Full Screen / Esc

Printer-friendly Version

Interactive Discussion

rohen@iup.physik.uni-bremen.de
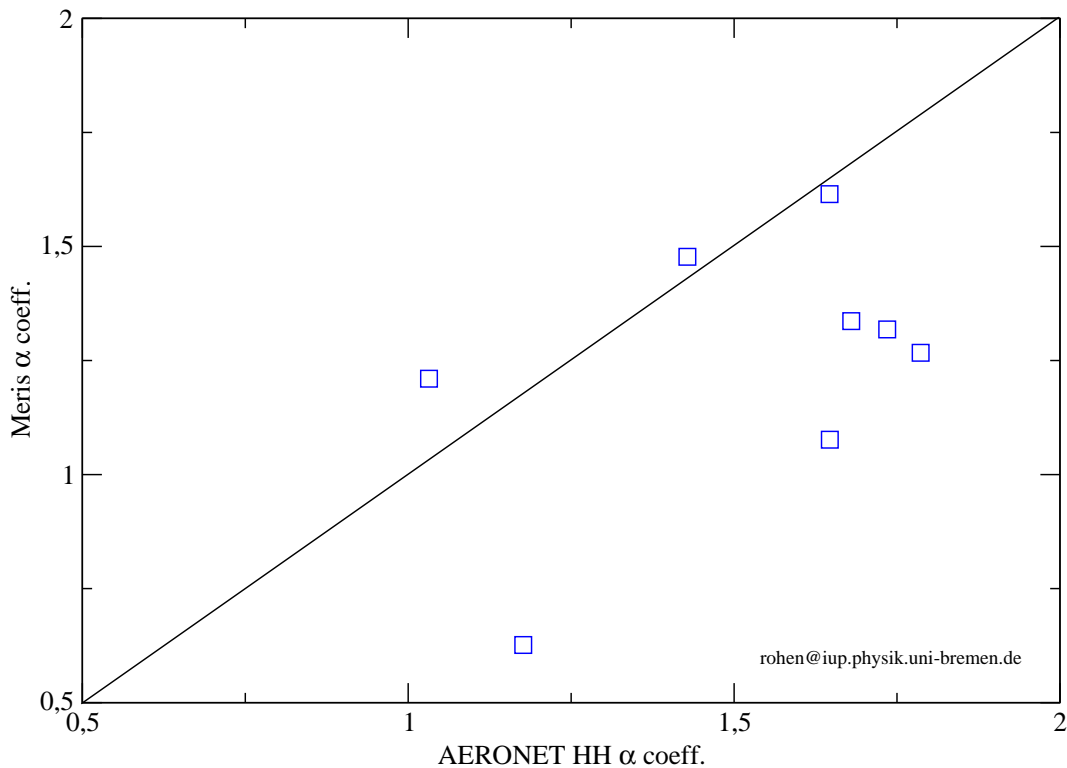
Fig. 9. Comparison of Ångstroem-α coefficient derived from respective aerosol optical depth at 440 and 675 nm from MERIS PMBAER and from AERONET L2 in Hamburg. Compared data have been arbitrarily chosen in 2005 and 2006 and deviate maximal 30 min in time and 300 m in space. Two measurements of AERONET are missing.

Fig. 10. Comparisons of PM$_{10}$ as retrieved from MERIS/PMBAER and national air quality measurements in Hamburg. The annotation denotes the gauging station and the site mode (BG=background, IND=industry, TRAF=traffic).
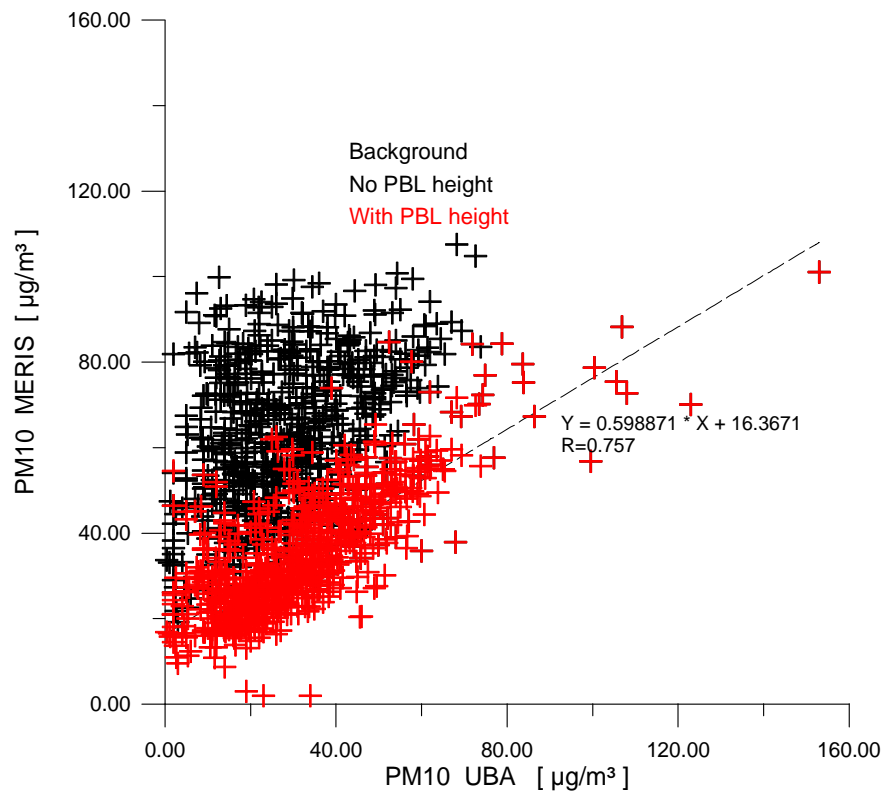
Fig. 11. Comparisons of PM$_{10}$ as retrieved from MERIS/PMBAER and national air quality measurements over rural sites in Germany, at 16 arbitrarily chosen sunny days in 2005 and 2006 (same as for the study over Hamburg), about 250 measurements have been compared. Validation results with and without using ECMWF boundary layer heights data show again that a PM$_{10}$ retrieval without the insertion of meteorological parameters is not possible. Figure has been taken from von Hoyningen-Huene et al. (2007b).
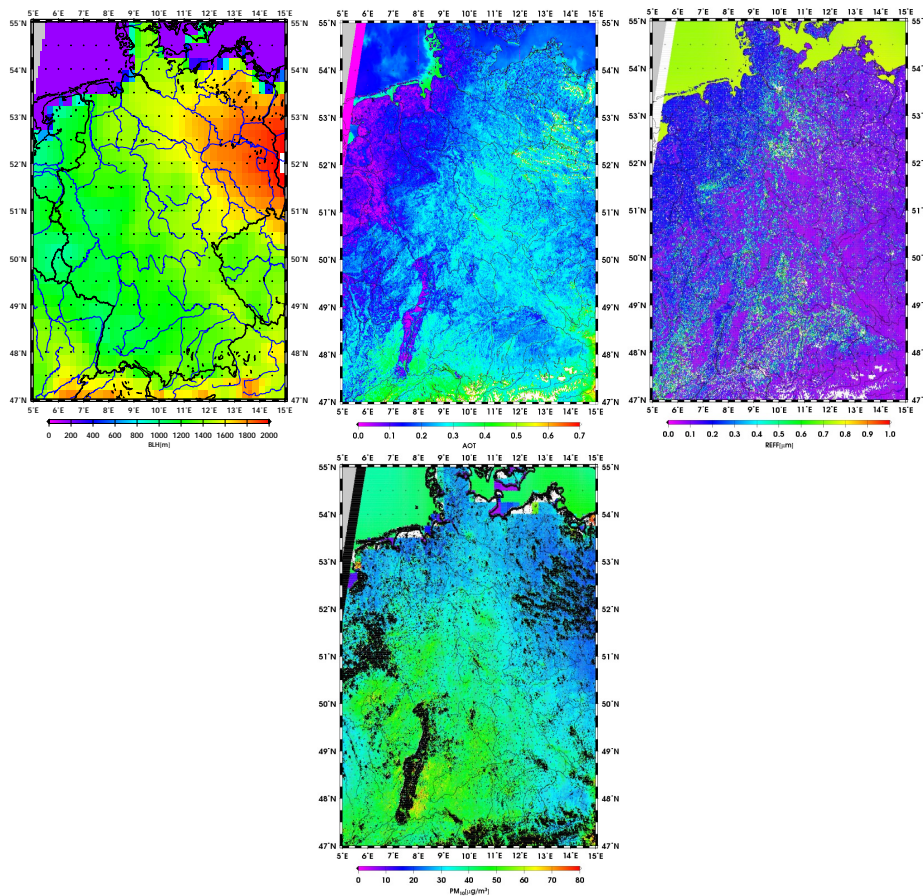
Fig. 12. Top left: Boundary layer height for 12 June 2006 over Germany as provided by ECMWF. Aerosol optical depth at 440 nm, effective radii and PM_{10} mass concentration as retrieved with PMBAER/MERIS. Retrieval was performed only over land.